

**Textures of geological materials: computer model  
predictions versus empirical interpretations based on  
rock deformation experiments and field studies**

Stefan M. Schmid, Geologisch-Paläontologisches Institut,  
Bernoullistrasse 32, 4056 Basel (Switzerland)

# **TEXTURES OF GEOLOGICAL MATERIALS**

Editors

H.J. Bunge, S. Siegesmund, W. Skrotzki, K. Weber

Edited by

Hans Joachim Bunge  
Institut für Metallkunde und Metallphysik  
Technische Universität Clausthal  
Clausthal-Zellerfeld, Germany

Siegfried Siegesmund  
Institut für Geologie und  
Dynamik der Lithosphäre  
Universität Göttingen  
Göttingen, Germany

Werner Skrotzki  
Institut für Kristallographie und  
Festkörperphysik  
Technische Universität Dresden  
Dresden, Germany

Klaus Weber  
Institut für Geologie und  
Dynamik der Lithosphäre  
Universität Göttingen  
Göttingen, Germany



INFORMATIONSGESELLSCHAFT • VERLAG

ISBN 3-88355-200-3

© 1994 by DGM Informationsgesellschaft mbH  
Adenauerallee 21, D-61440 Oberursel  
Alle Rechte vorbehalten  
Printed in Germany

Textures of geological materials: computer model predictions versus empirical interpretations based on rock deformation experiments and field studies  
Stefan M. Schmid, Geologisch-Paläontologisches Institut, Basel (Switzerland)

Abstract

Computer model predictions are confronted with texture analysis and interpretation of experimentally and naturally deformed rocks. It is emphasized that dynamic recrystallization plays a crucial role during texture evolution. Particular attention is given to simple shear deformation in ice, calcite and quartz materials which, in the presence of dynamic recrystallization, may lead to an end-orientation for easy slip in respect to one or several operative slip systems. It is concluded, however, that simple shear may be very rare in quartz-bearing mylonite belts.

Introduction

A recent review paper on deformation textures in rocks [1] emphasizes that texture interpretation needs to be based on physical principles and deplors that "although texture analysis has regained renewed popularity amongst geologists, it has in some ways regressed". Geologists are accused of "following a course depending either on plain intuition or simple geometrical constructions rather than well-founded physical concepts", the reason being that the complexities of the subject are "now commonly beyond the background of a structural geologist".

It is not the aim of this contribution to defend the geological community against such rude accusations. Instead, empirical evidence from rock deformation experiments and field studies will be reviewed in order to shed some light on an ongoing controversy: empirical interpretations seem to be at odds with certain predictions based on numerical modelling. First, a brief look at the results of texture modelling work is appropriate, work which is partially but not entirely based on well-founded physical concepts. Subsequently, this contribution will largely concentrate on empirical interpretations of textures formed during progressive simple shearing, as a result of "hot-working" in the presence of dynamic recrystallization.

It is interesting to note that Walter Schmidt [2] already realized that two alternative approaches towards texture analysis and interpretation are possible. One approach is an empirical one which he calls the "energetic" one ("der energetische Weg"). He empirically found that during texture development the lattice orientation of individual mineral grains tends towards a "low energy" position, i.e. an orientation which modern geologists describe as one of "easy slip", meaning that soft slip systems rotate into orientations with a high resolved shear stress. A second approach is referred to as the "mechanical" one ("der mechanische Weg"). It consists in analyzing the causes of lattice rotations and the exact path along which the lattice rotates into certain orientations. This is exactly what texture modelling attempts to do in a quantitative way. For obvious reasons experimental and field work meet with considerable difficulties in this respect (with the exception of in-situ experiments). However, we will see that these two approaches are comple-

mentary ones and that we will do little service to scientific progress by playing off one against the other.

#### Some comments on texture modelling work

Texture modelling work offers an excellent insight into how exactly texture development is influenced by the choice of active slip systems and associated critical resolved shear stress (CRSS) values, strain path (e.g. simple vs. pure shear) and type of finite strain (e.g. flattening vs. constriction). Additionally, it offers an opportunity to study the effects of certain simplifying assumptions about stress equilibrium ("lower bound" or "Sachs"-type models) and strain compatibility ("upper bound" or "Taylor"-type models). "Taylor"-type modelling (fig. 1a,b), first successfully applied to quartz [3,4], in fact offered

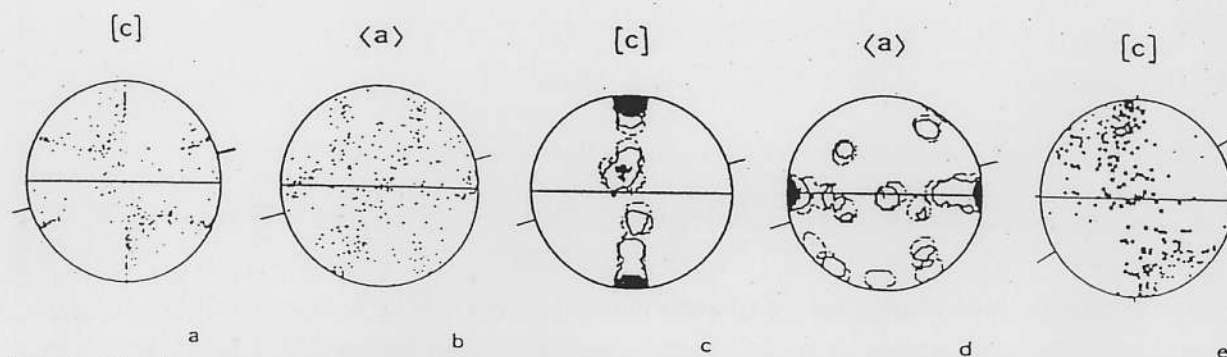


**Fig. 1:** Texture modelling of quartz deformed in dextral simple shear. The EW-reference line is the shear zone boundary (SZB), the ticks indicate the orientation of the flattening plane. Note that completely different c-axis pole figures (a,c,e) and a-axis pole figures (b,d) are obtained by using the same slip systems and ratios of CRSS-values (model C of [4]), but different models: Plastic rheology Taylor-type modelling in 1a,b after [4], modelling taking into account dynamic recrystallization in 1c,d after [12] and self-consistent viscoplastic modelling ( $n=3$ , work hardening) in 1e after [6].

extremely valuable insight into texture development while "Sachs"-type modelling, first applied to calcite [5], is inherently less powerful in handling different types of finite strain and strain path. One important result of this and subsequent modelling work based on these end-members is, that "Sachs"-type modelling results in a stable end-orientation (albeit not necessarily one of "easy slip") while "Taylor"-type models produce a dynamic equilibrium with high-density areas in the pole figure corresponding to orientations with a slow rotation rate. Thus, "Taylor"-type modelling does not predict stable end-orientations and is at odds with the empirical concept of an end-orientation of easy slip [1].

In the case of quartz a compromise between these end-members (called self-consistent modelling) was proposed. Different departures from purely plastic behaviour were admitted (viscoplastic rheology and work hardening), both for self-consistent and Taylor models [1,6]. Self-consistent modelling allows for heterogeneous strain. The effects of these modifications on the predicted c-

axis pole figures are rather dramatic in the case of simple shear: the single girdle c-axis pattern, often observed in quartzites deformed by simple shear, can only develop once the extreme assumptions behind "Taylor"-type modelling with plastic rheology invariably producing crossed girdles (fig. 1a) are modified (fig. 1e). Note, however, that the calculated c-axis single girdle (fig. 1e) is not perpendicular to the shear zone boundary (SZB). Hence, in spite of these modifications, no end-orientation for easy slip (associated with a c-axis girdle perpendicular to the SZB in the case of quartz deformed by simple shear) is predicted.

The models mentioned so far are largely, but not entirely based on physical principles (ultimately only finite element modelling will be able to provide a rigorous procedure, since certain parts of the programming procedure still are of an empirical nature). The principal value of this modelling work, as is the case for all modelling work in earth sciences, is to show exactly how certain assumptions influence the final result. Unfortunately field geologists and, occasionally, the authors of modelling work themselves have a tendency to conclude that the assumptions behind the modelling work are correct once the product of modelling work resembles natural textures. It may be argued that an almost infinite number of combinations of slip systems, CRSS-values, degrees of departures from purely plastic behaviour is likely to eventually produce the desired result.

There exists another type of quantitative texture modelling work on a more empirical basis. Models of this group are essentially geometrical models rather than being mechanical ones. Strongly heterogeneous strain and/or dynamic recrystallization are taken into consideration. Early modelling by Etchecopar [7] is inspired by the observation that minerals often have less than five independent slip systems active, as is required for strain compatibility. It is important to note that compatibility is only partly achieved in this type of model and that lattice rotations are the result of rigid body rotations ("spin") of mineral grains rather than being the result of compensatory rotations of the lattice resulting from shear-induced vorticity as is the case in "Taylor" type models [8]. Later, the Etchecopar model was extended to three dimensions [9] and the effects of recrystallization were simulated in a rather crude way: after a certain threshold strain, each mineral grain regains an equiaxed shape while preserving its lattice orientation. Both models of Etchecopar [7,9] do in fact predict an end-orientation for easy slip, as do the models discussed in the next paragraph.

Another type of modelling work is more realistic and takes into account specific recrystallization mechanisms. This modelling [10,11] is based on the "Taylor" end-member in terms of lattice rotations but it simultaneously allows for the effects of two mechanisms of dynamic recrystallization: subgrain rotation and grain boundary migration. This model, as was the case for the Etchecopar model and self-consistent models, again dramatically modifies the predictions of Taylor-modelling using a plastic rheology in that a single girdle c-axis patterns forms during simple shearing of quartz (fig. 1c,d). But, in contrast to the self-consistent model (fig. 1e) there is a pronounced tendency to form strong point maxima [12]. Furthermore, these point maxima correspond to end-orientations for easy slip for particular slip systems with a low CRSS value (fig. 1c). However, the slip systems in this favourable

orientation are not the only ones active. Also, the relative strengths of these maxima do not exactly match the chosen CRSS-values.

In summary, stable end-orientations can only be reached once dynamic recrystallization is taken into account. In the case of the Etchecopar model [7] the lattice rotations are still induced by spin and the effect of recrystallization is to relax the compatibility conditions. This latter effect is indeed to be expected in deformed rocks since the mobility of grain boundaries, or, in the case of subgrain rotation the creation of new grains, obviously must relax compatibility requirements. In the Jessell-model [10,11], however, lattice rotation is still entirely governed by the plastic Taylor model. The effects of recrystallization depend on the specific recrystallization mechanism. Fast grain boundary migration recrystallization prevalent at high temperatures leads to a volume increase of grains with a high CRSS and consequently low resistance to deformation. Such grains are assumed to have a low dislocation density and to be energetically more stable (note that the opposite, namely preferred growth of "hard" grains [18] has been experimentally observed for slow migration at very low temperatures). Subgrain rotation recrystallization, typical for intermediate temperatures, leads to the nucleation of new grains with an orientation controlled by old grains. In regard to both recrystallization mechanisms (slow migration not being considered) the Jessell model directly couples the effects of recrystallization to the Taylor-type predictions. The exact modes of this coupling were chosen rather arbitrarily. There are very close similarities between the Etchecopar and Jessell models in spite of the totally different modelling approach. This makes it obvious that a comparison between predicted and observed textures does not prove that particular assumptions behind any of the models are necessarily correct. However, the results of experimental and field studies discussed below will emphasize the role of dynamic recrystallization in promoting stable end-orientations.

#### Experiments in simple shearing

While there are numerous texture studies on geological materials deformed in uniaxial compression, laboratory studies performed under simple shear conditions, or conditions approximating simple shearing, are rare due to experimental difficulties. This is unfortunate since simple shear represents a particularly simple strain path and also has the advantage of experimentally achieving very large strains. It is important to note that simple shear is dissimilar to the rolling of metals. No shortening takes place in a direction perpendicular to the SZB (parallel to SD in Fig. 2) which at first sight might appear to correspond to the rolling plane. Furthermore, deformation is strictly plane strain (no length change in the "transverse direction"). Progressive deformation results in the rotation of the direction of finite extension (ED in fig. 2, equivalent to the flattening plane in three dimensions) towards parallelism with the shear direction (SD in fig. 2, equivalent to the SZB in three dimensions). Hence, progressive deformation of a polycrystalline aggregate according to the simple shear model is exactly analogous to progressive intracrystalline deformation of a single crystal due to slip on only one slip plane (parallel to the SZB) and parallel to one slip direction (the SD). From this it becomes obvious that a perfect end-orientation of easy slip of a single active slip system is only possible in the case of a single crystal which has an orientation of maximum resolved shear stress in respect to the

operative slip system (slip plane parallel to the shear zone boundary SZB, slip direction parallel to the shear direction SD). This being a highly idealized special case, we will merely have to discuss how closely one, or several, slip systems active in a polycrystal will be able to approximate end-orientations of easy slip. If they do, this has important consequences. For example, we may be able to infer active slip systems and deduce senses of shear from texture studies.

### *Ice*

Torsion experiments on ice [13] represent a particularly simple case illustrating that an end-orientation of easy slip in terms of, in this case, one predominantly active slip plane was indeed approximated to a great extent, but only after high strains and in the presence of extensive recrystallization by grain boundary migration. Basal slip in ice is reported to have a CRSS which is more than one order of magnitude lower than that of other slip systems [14,15]. With progressive simple shearing (fig. 2a,b) a transition from two c-axis maxima towards a single maximum is observed. The single maximum centers around the position of an end-orientation of easy slip on the basal plane. This transition with progressive strain is analogous to the transition from a crossed girdle to a single girdle c-axis pattern in quartz, as predicted by modelling work once the effects of recrystallization are taken into consideration. The microstructure is characterized by prismatic subgrains and high grain boundary mobility. Prismatic subgrains indicate inhomogeneous strain. As will be pointed out below, fast grain boundary migration is taken to be responsible for favouring the evolving c-axis maximum perpendicular to the SZB [13]. These experiments almost exactly match data on natural shear zones in ice [16] which exhibit a gradual transition from a two-point maximum into a single point maximum with increasing shear strain (fig. 2d,e). Because "Taylor"-type and self-consistent models do not predict an end-orientation of easy slip and because the microstructure is dominated by extensive grain boundary migration recrystallization in both examples, the effect of grain boundary migration is inferred to be responsible for the texture evolution towards a single maximum. "Hard" grains, i.e. grains with a high CRSS, must have been preferentially consumed in the case of ice, as assumed by the modelling work of Jesell [10]. The presence of hard and soft grains implies heterogeneous stress on the grain scale, with dislocation densities being higher in hard grains. Note, however, that this finding is contrary to the postulate that "soft" grains may be more likely to be consumed [17] under certain circumstances (i.e. during "slow" grain boundary migration at lower temperatures, equivalent to "regime 1" recrystallization of [18]).

### *Quartz*

Experimental shearing in quartzites could only be approximated [19] in that substantial shortening normal to the SZB could not be avoided. In the case of a quartzite deformed under plane strain conditions (fig. 3c) up to a high shear strain  $\gamma=2.8$ , an asymmetric "girdle" with a point maximum approximately normal to the SZB and oblique to the flattening plane was observed (the measurements include old, i.e. non-recrystallized, grains only). However, as is the case in the low strain experiments on ice, a substantial portion of c-axes does not coincide with this maximum and tends to form a second maximum at

the periphery of the pole figure. This second maximum is more pronounced at a lower shear strain  $\gamma=1.3$  (fig.3b). Unfortunately this latter specimen was not

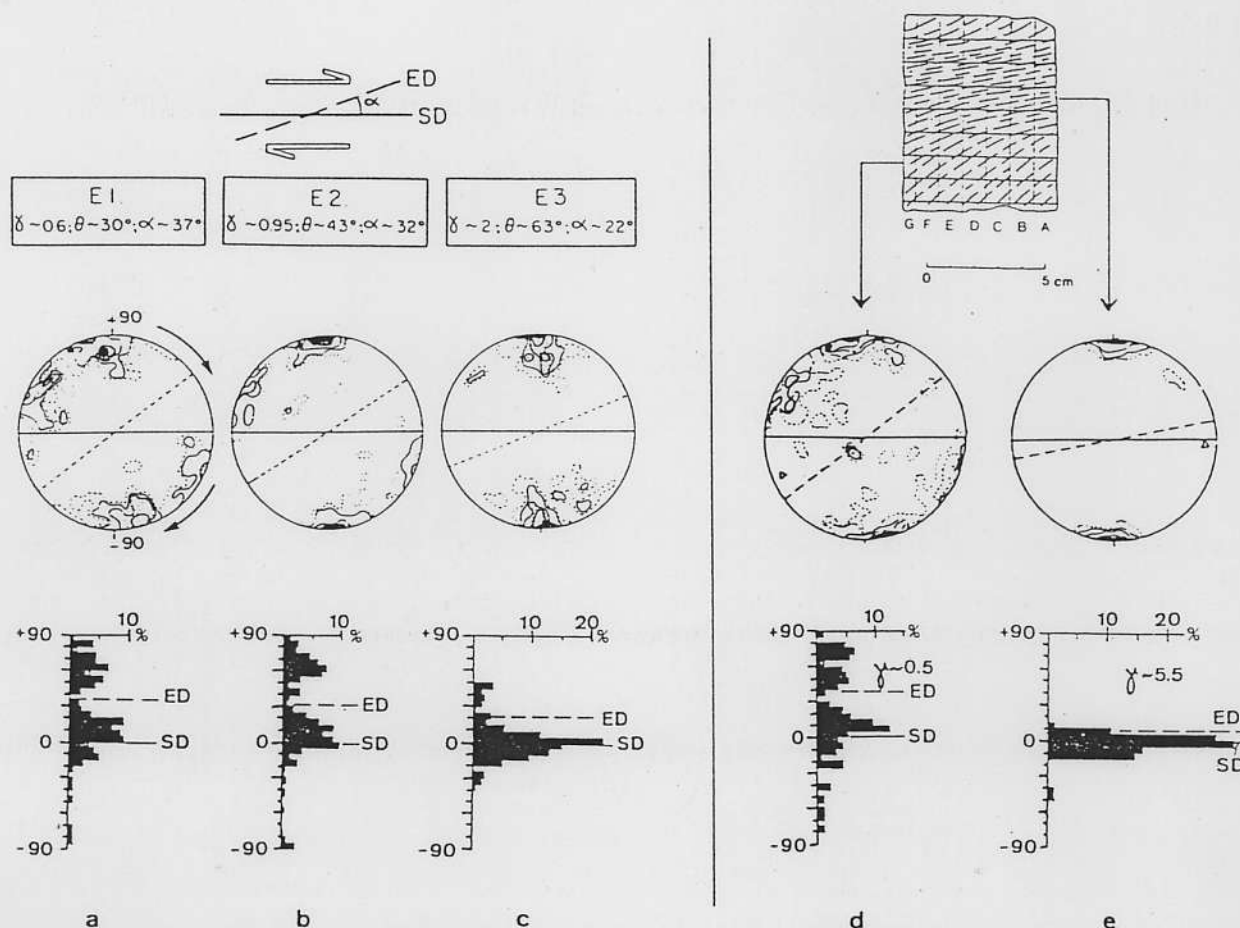
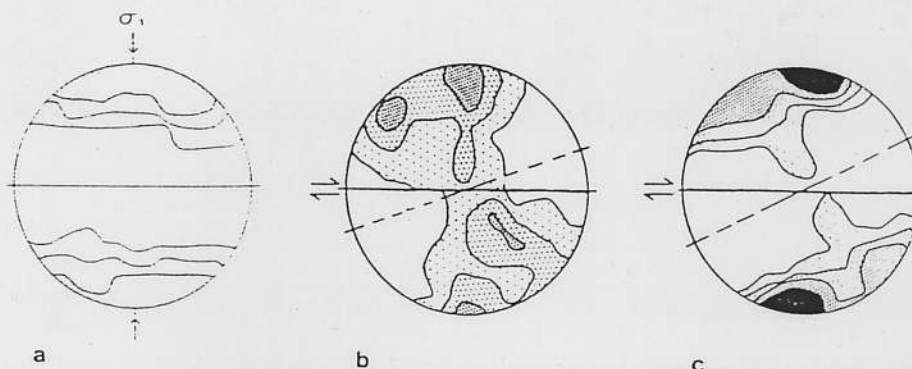


Fig. 2: The middle row exhibits c-axis pole figures of experimentally (2a-c) and naturally deformed (2d-e) ice under conditions of dextral simple shearing, after [13, 16]. The EW-reference line is the SZB, broken lines indicate the orientation of the flattening plane. Shear strain increases from  $\gamma=0.6$  to  $\gamma=2$  in 2a to 2c and from  $\gamma=0.5$  to  $\gamma=5.5$  in 2d to 2e. The top row (left) sketches the orientation of the flattening plane (ED) and the shear direction (SD, parallel to the SZB in three dimensions),  $\alpha$  is the angle between flattening plane and SZB, decreasing with increasing angle of shear  $\theta$ . The top (right) sketches the natural shear zone in ice, from which the pole figures 2d-e have been extracted. The bottom row plots histograms which relate to the c-axis pole figures: the azimuth of the c-axis positions is plotted in respect to the azimuth of the shear zone boundary (solid line labelled SD) and the azimuth of the foliation (broken line labelled ED). Note how the two maxima amalgamate into a single maximum parallel to the shear zone boundary with increasing strain.

deformed under plane strain conditions, therefore it is not directly comparable to the specimen depicted in fig. 3c. However a comparison with other pole figures produced under conditions departing from plane strain [19] suggests that the transition from a type I crossed girdle (fig. 3b) towards a

single girdle (fig. 3c) is primarily due to the increasing shear strain, analogous to the findings in experimentally deformed ice. Another study of experimentally produced shear zones in quartzites [20] approximates simple



**Fig. 3:** C-axis pole figures of experimentally deformed quartzite after [19] based on U-stage measurements on old non-recrystallized grains. The EW-reference line is the plane of flattening in 3a, but represents the SZB in 3b,c, with the flattening plane indicated by the broken line. Fig.3a: uniaxial compression; fig.3b: dextral shear strain  $\gamma=1.3$ , combined with 17% shortening across the SZB under non-plane strain conditions; fig.3c: dextral shear strain  $\gamma=2.8$ , combined with 46% shortening across the SZB under plane strain conditions.

shear to an unknown extent since shear zones formed in response to strain heterogeneities during bulk uniaxial shortening. Despite the poorly constrained experimental conditions, the c-axis single girdles are similar to that depicted in fig.3c.

Unlike the case of ice, textures in experimentally deformed quartzites cannot be interpreted to strongly approximate end-orientations of easy slip in terms of one predominant slip system. In the case of fig. 3, basal slip was inferred to be predominant under the chosen experimental conditions [19]. Due to the complicated strain path departing from simple shear as well as due to the lack of information on crystallographic directions other than the c-axis, the possibilities of an empirical interpretation are rather limited. Nevertheless, a marked asymmetry of the texture in respect to the flattening plane evolves, an asymmetry which is best explained to result from a tendency of the basal planes to rotate towards the SZB, i.e. away from a position normal to the flattening plane characteristic for uniaxial compression under the same experimental conditions (fig. 3a). On the other hand, these experiments confirm the validity of using such asymmetries as sense of shear criteria, as previously proposed by many authors based on field observations [21].

### Calcite

In regard to calcite, there are results for experiments performed under strict simple shear conditions, as well as from a complete texture analysis (via the calculation of an ODF from X-ray-data or from U-stage measurements) [22]. Hence, in contrast to ice and quartz, we are able to discuss the complete three-dimensional orientation of those crystals, which give rise to high-

density areas in a pole figure or in three-dimensional representations (ODF). Such orientations may be referred to as "texture components" [1] or "favoured crystal orientations" [22]. It is absolutely correct, that such an exercise is of a geometrical nature in that it merely helps in visualizing an orientation distribution and, consequently, does not lead to an immediate physical interpretation [1]. However, we will see that an interpretation based on the OFD nevertheless offers valuable insight into mechanisms of texture formation.

A first example concerns fine-grained limestone, experimentally deformed at 500°C [22] up to a shear strain  $\gamma = 1.22$  (ST 2 in fig. 4). Virtually identical textures have also been found by other authors [23] for fine-grained limestone deformed under similar experimental conditions. Three maxima are observed at the margin of the c-axis pole figure, labelled 1,2,3 in fig. 4a. Maximum 1 yields a favoured crystal orientation with a basal plane in an orientation of high resolved shear stress, slightly off the SZB in a counterclockwise sense. Maximum 2 consists of 2 submaxima (2a, 2b in fig. 4b,c), corresponding to orientations of high resolved shear stress in respect to r- and f-slip respectively, again slightly off the SZB in the same sense. The same holds for maximum 3, this time with respect to negative slip on an r-plane. Many other workers [5,23,24] concluded r and f to be the dominant slip systems operative at these temperatures and strain rates from independent evidence. Therefore, it must be concluded that these two active slip systems are found in orientations of high resolved shear stress, albeit not exactly coinciding with an "ideal crystal orientation" for simple shear. However, maximum 1 yields such an orientation in respect to the basal plane. Hence, it was inferred that basal slip was active as well [22]. Evidence for the existence of basal slip has been found in naturally deformed calcite [25] and postulated in the case of a high temperature texture discussed later (bottom row of fig. 6). The strong preferred alignment of r, f and basal planes, as well as the preferred alignment of the respective slip directions with the SZB and the SD, is directly visualized in the inverse pole figures in respect to these two unique specimen directions (fig. 4d): the normal to the SZB forms three maxima near c, r and f, while the SD forms two maxima near a and the slip direction for r and f (s.d. in fig. 4d).

Because of the systematic counterclockwise deflection of all the three inferred slip planes in respect to the SZB during simple shear, strain compatibility requires antithetical slip to occur in a plane at a high angle to the SZB (see fig. 10a in [26], and fig. 10, second sketch from the left). This is exactly the case for r, f and the basal plane in the case of the favoured crystal orientations corresponding to maxima 2b, 2a and 3, respectively (fig 4c). The calculated pole figure for the slip direction common to both r and f indeed exhibits two maxima at the margin of the pole figure, supporting the interpretation of conjugate slip, with a subordinate antithetic system leading to a second and weaker maximum at a high angle to the SZB. From this it is concluded that, in this case, an ideal crystal orientation is only crudely approximated.

It is interesting to note that this empirical interpretation leads to similar results when compared with another interpretation of the same texture based on Taylor modelling [27]. There is one important difference in interpretation however: Taylor modelling incorporated e-twinning in addition to r- and f-slip. In contrast to this, there is no microstructural evidence for e-twinning to have

been operative at all in ST 2 (fig. 4). Moreover, the major effect of twinning on texture development would be rather dramatic in that twinning would create

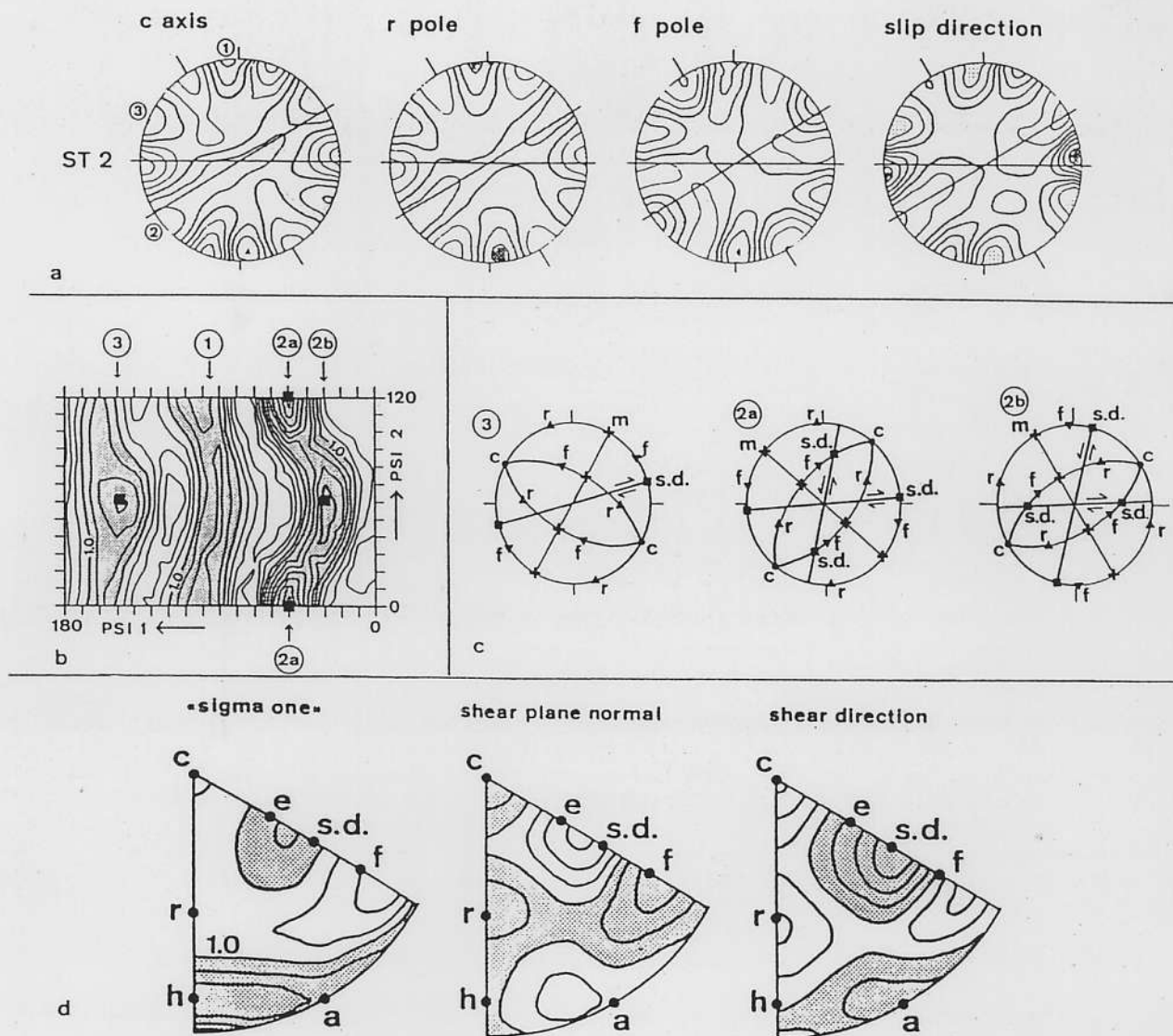


Fig. 4: Complete texture analysis of experimentally deformed Solnhofen limestone (dextral simple shear) after [22]. The EW-reference line is the SZB, the oblique line represents the flattening plane in case of the pole figure data. Fig. 4a: pole figure data for different crystallographic directions, "slip direction" refers to the zone of r and f slip planes and represents the slip direction common to both these slip systems. Fig. 4b: Section through the ODF at  $\text{PHI}=90^\circ$ , sampling all the information regarding c-axis positions on the primitive circle of the c-axis pole figure. Fig. 4c: Favoured crystal orientations for maxima 2a, 2b and 3 in Fig. 4a and b. Fig. 4d: Inverse pole figures for a direction at  $45^\circ$  to the SZB (sigma one), the normal to the SZB (shear plane normal) and the shear direction.

new crystal orientations corresponding to twinned domains [22], an effect not taken into account by Taylor modelling because Taylor modelling treats

twinning like an ordinary slip system. It is possible, that the introduction of basal slip might have yielded a similarity closer than that actually observed [27] between measured and calculated textures. Only 2 out of the 3 observed maxima are predicted by Taylor modelling (fig. 8 in [27]).

Numerical microstructural analysis of the sample in discussion yielded grain shapes exactly corresponding to the imposed strain [22]. Hence in this case grain boundaries behaved like passive marker lines and processes of recrystallization can be excluded. Very probably, it is the absence of recrystallization which prevents the formation of a texture approximating an end-orientation for easy slip, in accordance with the predictions based on Taylor-type or self-consistent modelling.

Recrystallization by the subgrain rotation mechanism was active in a specimen of Carrara marble (CT 6, top row) deformed at 700°C up to a large shear strain of  $\gamma = 2.85$ . The c-axis pole figure of this specimen (fig. 6, top row) exhibits the same 3 maxima (labelled 1,2,3) as previously described for ST 2 (fig. 4a). This time the r and f planes as well as the basal plane are perfectly aligned with the SZB within measurement error. The slip direction of r and f is parallel to the shear direction. Hence, the orientation of these active slip systems is in an end-orientation for easy slip. Of course, only one of them can be aligned with the SZB within one individual grain. All this implies a change of the operative slip system from grain to grain, and additionally, heterogeneous deformation on the grain scale.

How can such an end-orientation for easy slip be achieved? Numerical microstructural analysis of grain shapes in this specimen provided evidence that the cores of old grains were free to rotate due to "grain boundary sliding" in the sense that displacements across the recrystallized mantle regions occur [22]. Hence, this type of strain partitioning allows for rigid body rotations (spin) of elongated old grains. Such rigid body rotations are not taken into account by Taylor-type modelling, in contrast to the Etchecopar model discussed earlier. It is proposed that these rotations may allow for an end-orientation in respect to the active slip systems to develop.

Carrara marble (CT 7) deformed at 800°C to a similar shear strain ( $\gamma = 2.74$ ) is completely recrystallized by fast grain boundary migration recrystallization associated with grain growth (fig. 5a). The c-axis pole figure (fig. 6, bottom row) is analogous to that of ice (fig 2,a,b,d) in that the basal planes are almost perfectly aligned with the SZB, the  $\langle a \rangle$ -slip direction being aligned with the shear direction (maximum 1 in fig. 6). Only a few grains correspond to a second maximum (maximum 2 in fig. 6), interpreted to have resulted from basal slip in an antithetic sense. Since the pole figures for r, f and the slip direction of r and f do not show the distinct preferred orientation exhibited by CT 6, it was concluded that this specimen deformed by single slip along the basal plane [22].

The microstructural analysis of CT7 (fig. 5a) makes it clear that the grain boundaries are extremely mobile. Hence, compatibility between neighbouring grains is always given even if deformation is inhomogeneous on a grain scale. The extremely strong texture is interpreted to result from the preferred growth of grains in an end-orientation for easy slip on the basal plane. Hence,

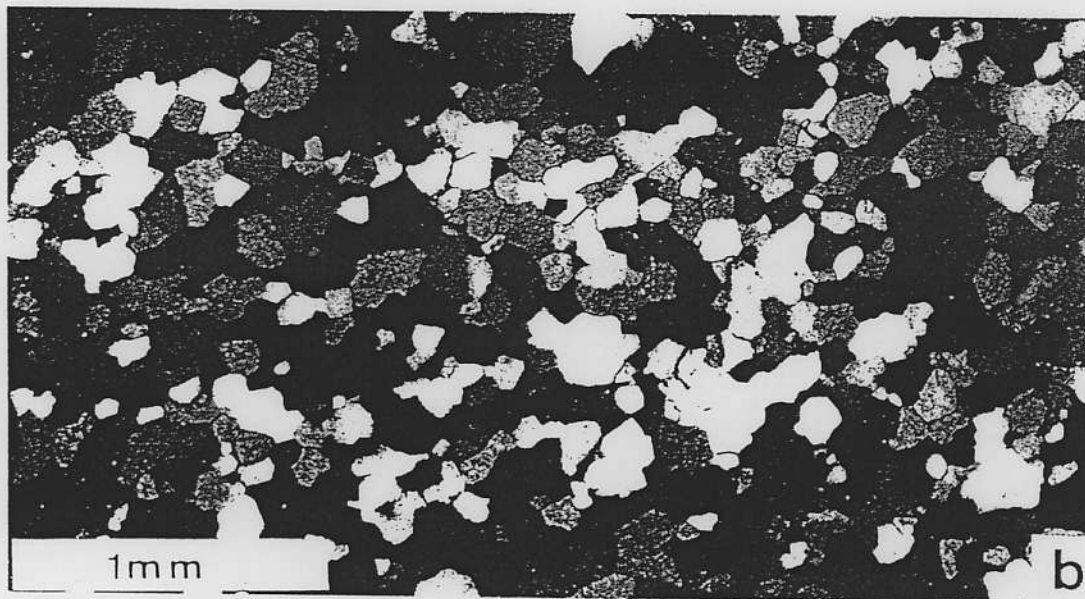
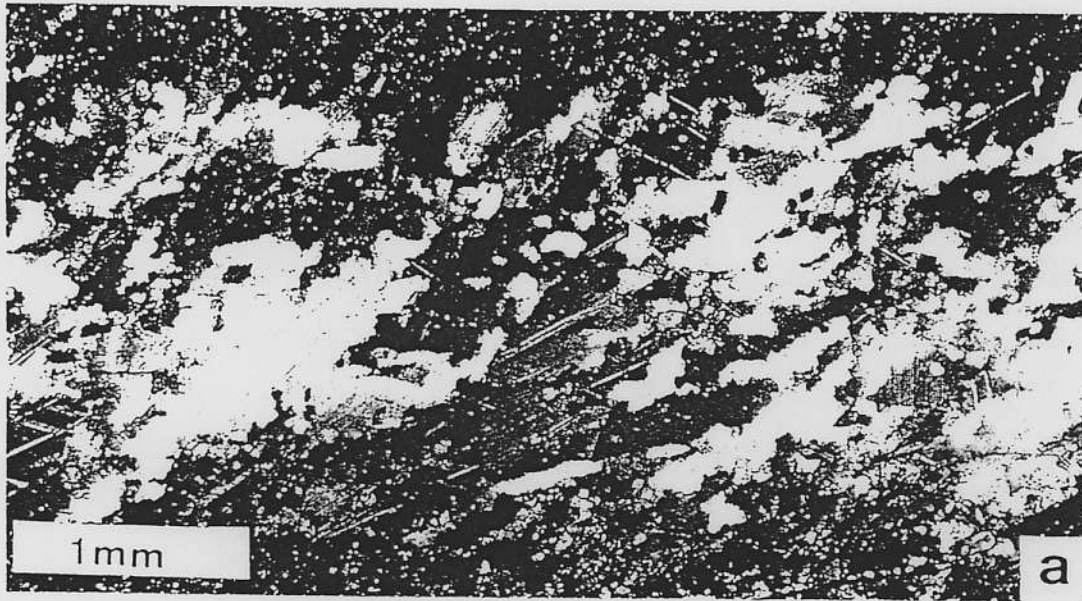


Fig. 5: Dynamic recrystallization in experimentally deformed Carrara marble CT7 (5a, compare texture in fig. 6, bottom row) and naturally deformed quartzite CC1 (5b, compare texture in fig. 7). Grain boundary migration recrystallization produces highly irregular grain shapes in the case of CT7 (fig. 5a). All dark grains closely coincide with maximum 1 in Fig. 6, bottom row, hence their basal planes are sub-parallel to the SZB (horizontal in 5a). Syntectonic recrystallization in CC1 (fig. 5b) leads to relatively well-equilibrated grain boundaries. Note that in both cases grain shape is far from reflecting the total strain. The sense of shear is dextral for both specimens.

as was the case for ice, it is the creation of new volume of grains in a "soft" orientation (high CRSS) which governs texture evolution.

In conclusion a comparison between the three calcite textures discussed here reveals that: (i) As predicted by Taylor modelling an end-orientation of easy slip does not evolve in the absence of recrystallization. Instead, a preferred

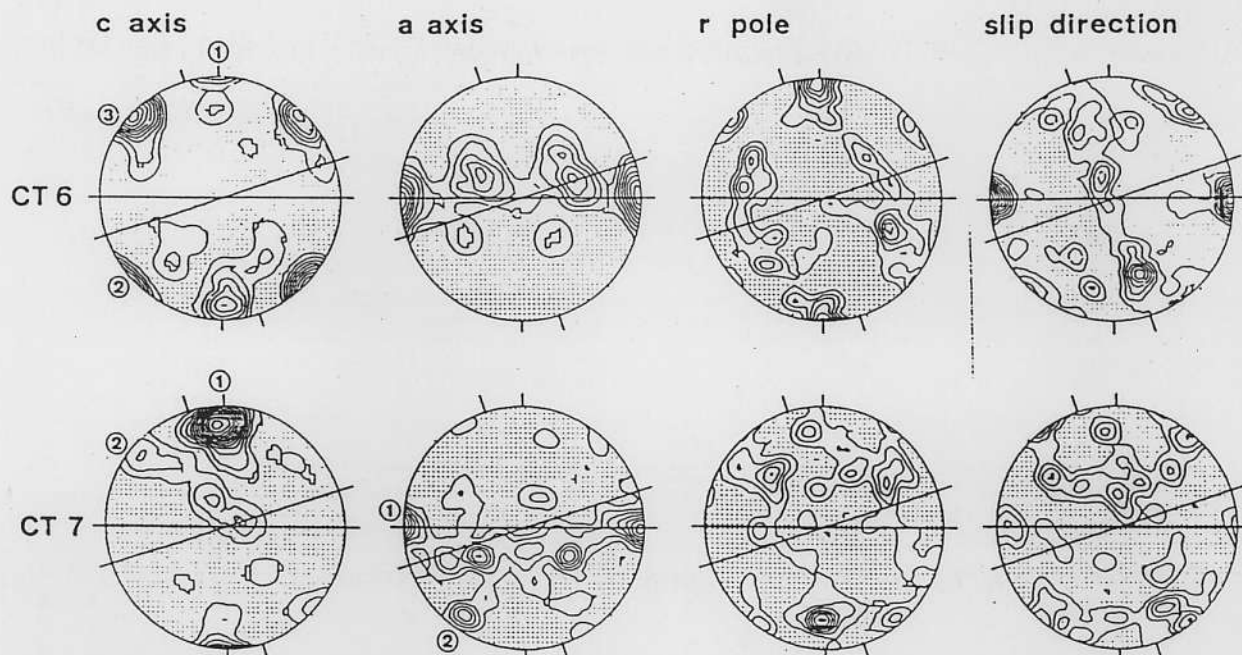


Fig. 6: Pole figures for Carrara marble experimentally deformed in dextral simple shear. The EW reference line is the SZB, the flattening plane is indicated by the oblique line. The top row refers to Carrara marble deformed at 700°C, where rotation recrystallization dominates, the bottom row to Carrara marble deformed at 800°, where migration recrystallization dominates.

orientation in terms of conjugate antithetic slip with high resolved shear stress on the active slip systems is observed. (ii) An orientation for easy slip does evolve in the presence of recrystallization. In the case of subgrain rotation recrystallization old grains are allowed to spin, while in the case of fast grain boundary migration recrystallization preferential growth of soft grains is predominantly responsible for texture formation. (iii) The analysis of texture components is a useful tool for inferring active slip systems.

#### Field studies

Applications of texture analysis in regard to solving various research problems in structural geology have recently been reviewed [28]. This contribution will mainly concentrate on two natural examples of quartz textures in order to discuss the role of dynamic recrystallization in regard to texture formation, and discuss if and how we can extract information on active slip systems, the type of finite strain and the strain path from texture studies.

### *A natural example of deformation in simple shear*

Only in very rare cases is it possible to gain independent information on the displacement gradient tensor, i.e. the exact strain path. Simple shear (or better, simple shearing [29]) is a particular strain path along which lines parallel to the shearing direction do not change their length. Generally the only traces of deformation visible in a rock deformed by simple shear are the foliation, believed to represent the flattening plane, and the stretching lineation. While pole figures of rocks experimentally deformed in simple shear were presented with respect to the SZB (i.e. a kinematic reference frame), pole figures from naturally deformed rocks have to use the foliation and stretching lineation (i.e. strain axes) as a reference frame. In rare cases, however, additional information is available and the texture of quartz specimen CC1 [30] is one of these cases.

CC1 is a deformed quartz vein. The parallel-sided walls of this quartz vein are deflected towards parallelism with the shear zone boundary (fig. 7a). Assuming no volume change, it is possible to find the direction along which the width of the vein does not change (i.e. the direction parallel to the shear zone boundary) if the vein underwent simple shearing. Such a direction can be indeed found in the case of CC1 and the shear strain  $\gamma$  was inferred from the angle between the foliation and the SZB.  $\gamma$  varies between 3.2 and 6.2 within the analysed specimen, the foliation being curved within the measured domain.

The microstructure of this deformed quartzite vein is characterized by nearly equant grains in spite of the very large strain (fig. 5b). Assuming the mineral grains to deform homogeneously in the absence of recrystallization, individual grains would be flattened to an aspect ratio of 11 (for  $\gamma=3.2$ ) and 40 (for  $\gamma=6.2$ )! Again, compatibility between grains is obviously no issue, since grain boundary mobility is so high that an equilibrium "foam" microstructure is continuously re-established during deformation. In the low strain part of this shear zone this stable grain size is seen to evolve through syntectonic recrystallization, hence it cannot represent the result of post-tectonic annealing. We do not know the exact mechanism by which grain boundary migration (or possibly grain boundary sliding) maintaining the foam structure influences texture development. But, as was the case in the experimentally deformed examples exhibiting stable end-orientations (ice and calcite), recrystallization appears to play a key role in the development of such an end-orientation for easy slip.

Fig. 7b represents the c-axis pole figure with the mean orientation of the foliation within the analysed specimen (fig. 7a) oriented E-W, the inferred normal to the SZB and the SD being labelled A and B, respectively. The c-axis pole figure represents a quartz single girdle oblique to the strain coordinate system, indicating dextral shear. From the calculated ODF favoured crystal orientations have been extracted for particular c-axis positions along this single girdle by a procedure analogous to that illustrated in fig. 4. The following picture emerges: one  $\langle a \rangle$  direction lies approximately in a constant orientation parallel to the shear direction B while the c-axes are free to be located anywhere along the single girdle. In c-axis position 1 the basal plane is aligned with the SZB (fig. 7c) while positions 2-4 and 6-8 have a positive rhomb  $r$  and position 5 has a first order prism  $m$  close to the SZB, respectively.

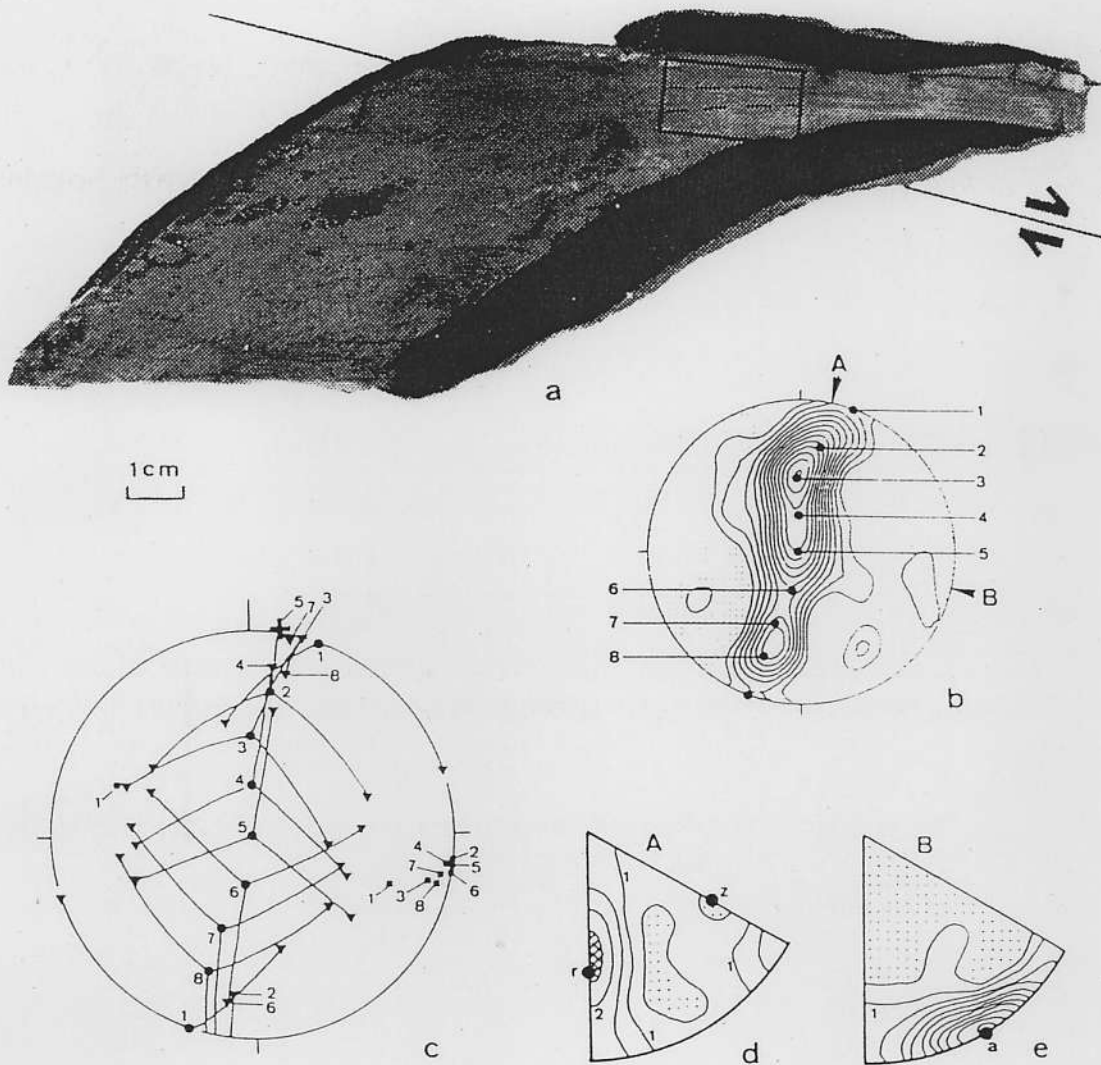


Fig. 7: Texture analysis of a quartzite (CC1), naturally deformed under conditions of dextral simple shear, after [30]. Fig. 7a: Hand specimen with the frame indicating the analysed specimen, the broken lines indicating the foliation trace and the solid line the SZB. Fig. 7b: c-axis pole figure (EW-reference line indicates the average orientation of the foliation within the analysed specimen) and numbering of selected c-axis positions (compare with fig. 7c), the directions A and B corresponding to the normal to the SZB and the SD, respectively. Fig. 7c: Selected favoured crystal orientations. Fig. 7d: Inverse pole figures for the normal to the SZB (direction A). Fig. 7e: Inverse pole figure for the shear direction SD (direction B).

Conversely, looking at the inverse pole figures for the kinematic directions A and B (fig. 7d,e), we find the SD to align with  $\langle a \rangle$  (fig. 7e), while the normal to the SZB has a maximum at r, extending towards c and m (fig. 7d). From experimental work  $\langle a \rangle$  is a well established slip direction in quartz and the key role of a-axis pole figures in terms of kinematic inferences from field samples has been recognized for some time now [31]. In fact,  $\langle a \rangle$  appears to be the only operative slip direction in naturally deformed rocks such as CC1 and many others deformed at moderate metamorphic grades [30]. Only at very high temperatures has  $\langle c \rangle$ -slip been inferred, i.e. under granulite facies conditions [32] or during subsolidus deformation of granites [33]. In quartz, the  $\langle a \rangle$  slip direction is contained within the basal plane, the rhombs and the first order prisms. Hence, this texture of CC1 is most readily explained as one being very close to an end-orientation for easy slip in regard to all these slip systems (and others containing the  $\langle a \rangle$ -direction, see [34]). Alternatively, this texture may also be described in terms of pencil glide parallel to the  $\langle a \rangle$ -direction,  $\langle a \rangle$  being perfectly aligned with the shear direction of the simple shear zone.

#### *type I crossed girdles*

Relatively straight c-axis single girdles, such as discussed above, are relatively rare but other examples have been described and for a few of them simple shearing has been independently demonstrated [32,34]. More commonly transitional c-axis patterns ranging from kinked single girdles to asymmetrical and finally symmetrical type I crossed girdles [30] are observed (see fig. 9). Symmetrical type I crossed girdles are generally assumed to have formed during pure shear. Does this indicate that simple shearing is very rare during natural rock deformation and that transitions between simple and pure shear are very common? Before addressing the possible reasons for this transition, the other end-member, the symmetrical type I crossed girdle, will be discussed in terms of favoured crystal orientations.

Fig. 8a depicts a type I crossed girdle for specimen PT 463 [30], albeit slightly asymmetrical. The corresponding a-axis pole figure (fig. 8b) depicts two maxima of approximately equal strength,  $60^\circ$  apart from each other, symmetrically disposed about the foliation. A third, much weaker maximum is normal to the foliation. If  $\langle a \rangle$  is the only operative slip direction the position of a-axes at the primitive circle automatically implies plane strain conditions. Departures from plane strain are manifested by small circles of a-axes developing around the foliation normal (flattening field) or around the extension direction (constrictional field), hence the  $\langle a \rangle$  crystallographic directions are no longer restricted to point maxima on the primitive circle (see fig. 15 in [30]). This is consistent with the inference drawn earlier, namely that  $\langle a \rangle$  is the only major slip direction operative in quartz (except for very high temperatures where  $\langle c \rangle$  slip is observed).

The c-axis positions 4-10 form the central segment from which the crossed girdles branch off. This segment is straight because the individual quartz grains attempt to simultaneously place two of their a-axes into the maxima  $60^\circ$  apart. This, together with the "hexagonal" character of the ODF (no distinction between densities of positive and negative forms) in regard to positions 4-10 [30], is strong evidence for prism  $\langle a \rangle$  slip. Prism  $\langle a \rangle$  slip is able to simultane-

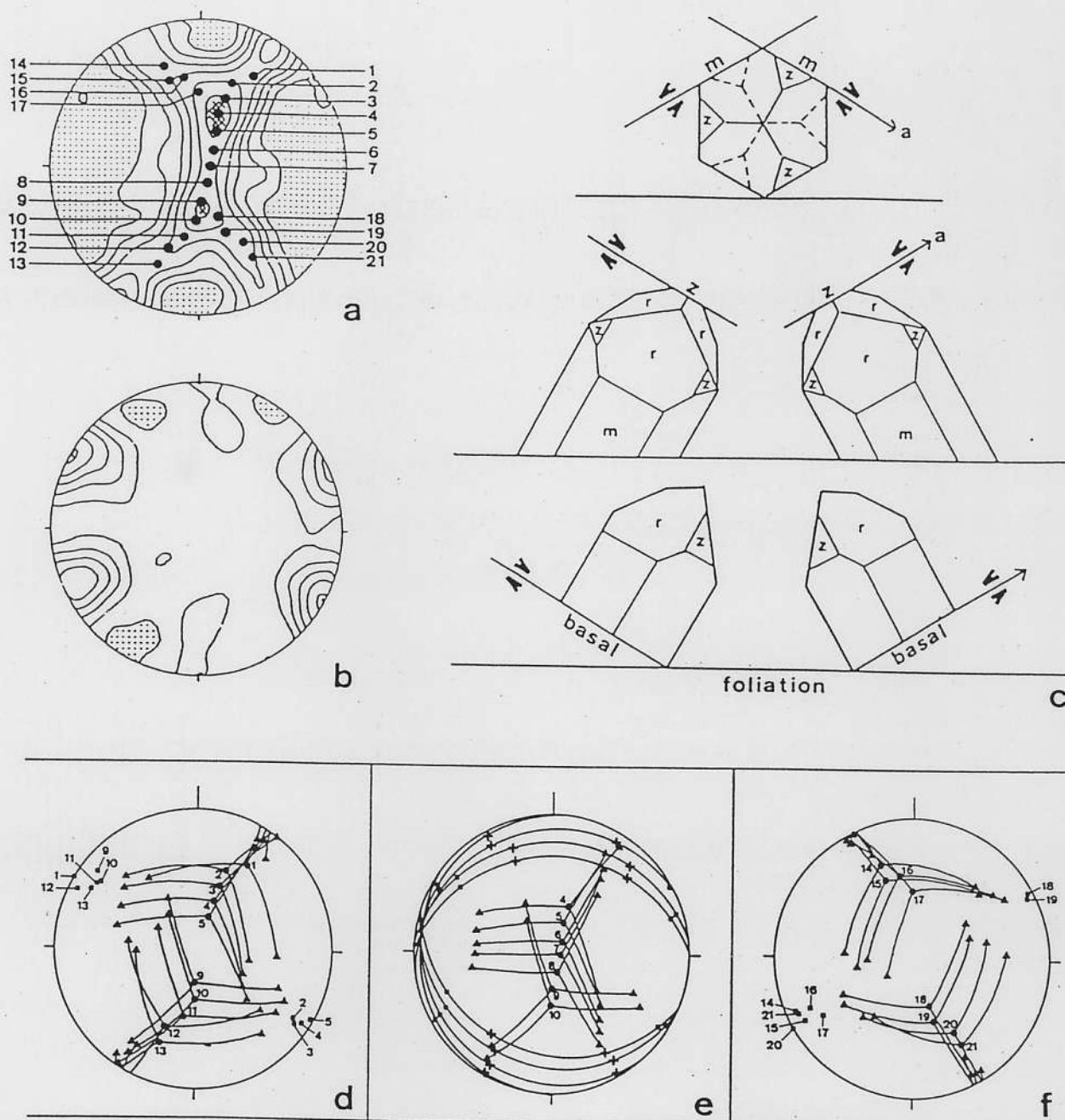


**Fig. 8:** Texture analysis of a naturally deformed quartzite (PT 463) exhibiting a typical type I c-axis crossed girdle. The E-W reference line indicates the orientation of the foliation, the lineation is at the margin of the pole figures. Fig. 8a: c-axis pole figure with selected c-axis positions. Fig. 8b: a-axis pole figure. Fig. 8c: view of the favoured crystal orientations extracted from figs. 8d-f. Fig. 8d-f: Favoured crystal orientations corresponding to the c-axis orientations indicated in fig. 8a.

ously operate parallel to two  $\langle a \rangle$  directions  $60^\circ$  apart (slip on two prism planes occurring in opposed or conjugate senses, Fig. 8c). For crystallographic reasons slip on the rhombs (in this case the negative rhombs z) can only operate parallel to one  $\langle a \rangle$ -direction within an individual grain (fig.

8c). Hence, each grain "has to decide" if it is going to glide parallel to one or the other of the  $\langle a \rangle$ -directions coinciding with the two maxima. As a consequence, the girdle splits into two separate legs in terms of the c-axis pole figure.

The leg characterized by positions 9-13 and 1-5 (fig. 8d) has the same characteristics already discussed for the single girdle texture of CC1 in terms of favoured crystal orientations (except that z replaces r). Furthermore, the second leg (positions 14-17 and 18-21) forms a mirror image of the first (fig. 8f). Hence, strain is partitioned into shearing in two opposed senses. It is very important to note that, in this case, each grain can only slip in a dextral or a sinistral sense. Hence, deformation on the grain scale must be heterogeneous. This manifests itself occasionally by the development of fabric domains, which are best visualized by the axial distribution analysis, the "Achsenverteilungsanalyse" of Sander [35]. In case of the specimen described here, about 50% percent of the grain volume is dynamically recrystallized, and it is again primarily the effect of recrystallization which relaxes compatibility requirements. On the scale of the mineral aggregate as a whole, i.e. the rock, simultaneous conjugate slip parallel to the two  $\langle a \rangle$ -directions symmetrically disposed to either side of the stretching lineation, will lead to non-rotational (pure shear) deformation in case of a strictly orthorhombic symmetry of the texture.

Of course many of the arguments proposed in favour of the empirical interpretation given above are of a geometrical nature. However, it is very hard to deny the fact that the favoured crystal orientations extracted from the ODF, i. e. the texture components, represent favoured crystal orientations with a high critical resolved shear stress on experimentally documented slip systems. On the other hand, it is remarkable that similar type I crossed girdle c-axis pole figures have been simulated by Taylor-type modelling ([4] and fig. 1a). Taylor-type modelling assumes homogeneous strain on the grain scale, it incorporates  $\langle c+a \rangle$  slip, for which we found no empirical evidence and it does not predict end-orientations. Therefore it is inferred, that the similarities are due to an appropriate choice of CRSS-values ultimately leading to the desired result in terms of a c-axis pole figure. The marked differences between observed (fig. 8b) and modelled a-axis pole figures [4] show that the close similarities between model prediction and nature are restricted to c-axis pole figures.

*The transition from type I crossed girdles to a single c-axis girdle, or, how common is simple shear in mylonite zones?*

Quartz textures reported from mylonite zones cover a wide spectrum of c-axis pole figures ranging from c-axis single girdles over asymmetrical crossed girdles to near-orthorhombic crossed girdles (top row in fig. 9). This has been used to qualitatively [36] and quantitatively [37] assess the strain path during plane strain deformation in terms of the vorticity of deformation [38], simple shear and pure shear being the end-members considered in this discussion. This is not an easy task for several reasons:

Firstly, the operative slip systems and the type of finite strain (plane strain, constriction, flattening) also have an influence on the resulting texture [4, 30]

and the effects of these factors have to be taken into consideration before discussing vorticity. In the case of quartz the predominance of  $\langle a \rangle$  slip under most metamorphic conditions has been discussed above. Hence the predominance of particular active slip systems containing the  $\langle a \rangle$ -direction leads to different patterns of c-axis densities along single or crossed girdles. These girdles are oriented perpendicular to one or two a-axis maxima, the a-axis pole figures playing a key role in the interpretation. In this sense girdles may degenerate into maxima along the girdles. For example, c-axis maxima parallel to Y or in the primitive circle can simply be taken as cases where basal

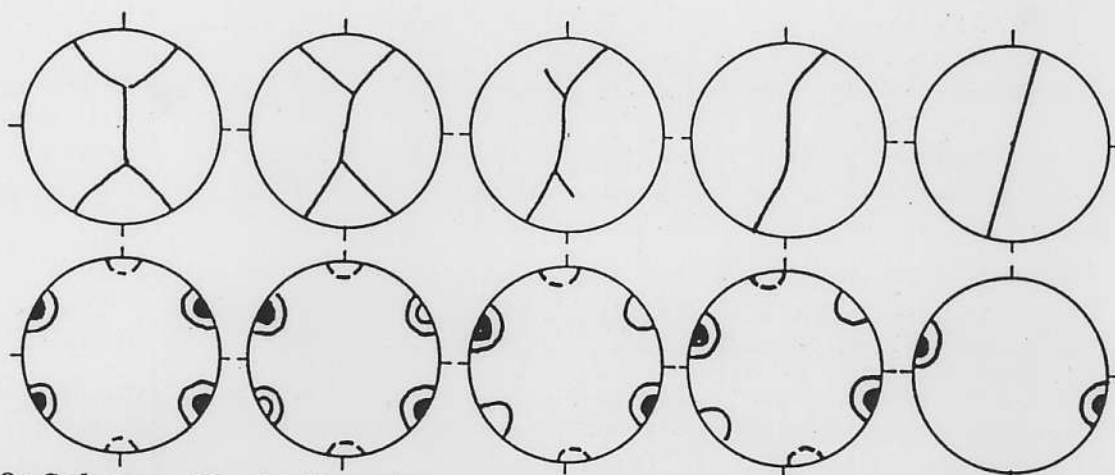


Fig. 9: Scheme illustrating the transitional stages from a c-axis single girdle (top row to the right) to a type I symmetrical c-axis crossed girdle (top row to the left), and associated a-axis pole figures (bottom row) after [30]. In this contribution this transition is interpreted to reflect a transition from simple shear (right) to pure shear (left).

or prism slip, respectively, predominate. Departures from plane strain conditions are again best assessed by looking at the a-axis pole figure. In the following we will concentrate on quartz textures exhibiting a-axis maxima contained in the primitive circle of the a-axis pole figure (as illustrated in fig. 9, bottom row).

Secondly, theoretically there are two possibilities for explaining the transition from crossed girdles to single girdles, given plane strain conditions and regardless of the active slip planes [30]. The transition may indeed indicate increasing vorticity towards the end-member of simple shear. Alternatively, it may simply reflect the increasing influence of recrystallization with progressive deformation at a given vorticity number. For example, increasing deformation and recrystallization under simple shear conditions may lead to such a transition as observed in the experiments on ice discussed earlier. Modelling work has indeed demonstrated that crossed girdles may also form during simple shear, albeit asymmetrical in respect to the foliation (fig. 1a). Experimental work on ice (fig. 2c,e) and calcite (fig. 6), on the other hand, demonstrated that parallelism between the SZB and the predominant slip systems can be achieved in the presence of recrystallization.

What about quartz textures measured in naturally deformed quartz? Unfortunately we rarely have independent evidence on the kinematic framework such as was the case for CC1. Three arguments may be raised in favour for interpreting this textural transition to be due to an increasing vorticity number, i.e. a transition from pure shear to simple shear:

(1) In cases where independent evidence for simple shearing can be provided, single girdles have in fact been observed [32,34].

(2) Strain in mylonite belts is by definition very high and syntectonic recrystallization is invariably involved in the formation of mylonites from which such transitions have been described. In analogy to the experiments, large strains and abundant syntectonic recrystallization are expected to lead to single girdles in the case of simple shear. In spite of this, many crossed girdles (often only slightly asymmetrical) are reported from extensively recrystallized quartz-bearing mylonites.

(3) In the case of mylonites associated with asymmetrical crossed girdles, the angle between the dominant a-axis maximum and the foliation is larger than the "expected" angle ( $\alpha$  in fig. 2 and fig. 10) between the foliation and the SZB.

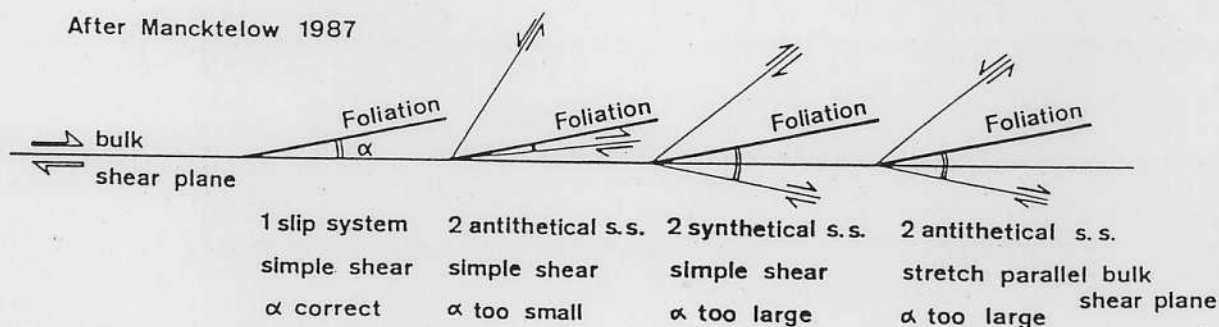


**Fig. 10:** This diagram is redrawn after fig. 10 in [26]. It depicts highly idealized sketches to illustrate how total strain in the specimen can be partitioned into slip on individual intracrystalline glide planes. The angle  $\alpha$  is defined as the angle between foliation and SZB (or "bulk shear plane"). If only one slip system operates and if this slip system is aligned with the bulk shear plane (left hand sketch), the angle  $\alpha$  may be correctly inferred from the angle between a-axis maximum and foliation. The other three sketches illustrate the simultaneous activity of two slip systems (in reality two a-axis maxima in the pole figures). If the angle  $\alpha$  would be inferred from the angle between the dominant a-axis maximum (represented by the slip system at a small angle to the bulk shear plane in these sketches) and the foliation, this angle would turn out to be "too small" or "too large" in respect to the simple situation depicted in the left hand sketch. See text for further discussion.

The angle  $\alpha$  depends on the shear strain  $\gamma$  according to  $\tan 2\alpha = 2 / \gamma$  and amounts to a few degrees only at large shear strains. An angle of  $20^\circ$  or even more is commonly observed between a-axis maximum and foliation. "Expected" in the context of the angle  $\alpha$  means that the a-axis maximum

should be parallel to the SZB provided an end-orientation of easy slip is reached during simple shear. The experiments on calcite showed that, during simple shear deformation, the operation of a second set of favoured crystal orientations in an antithetic sense (fig. 4 and fig. 10, second sketch from the left) has an opposite effect in that the inferred angle  $\alpha$  is too small: the departure of the favoured crystal orientation of the dominant and synthetically operating slip systems is towards the foliation and away from the SZB. Hence, the inferred angle  $\alpha$ , as measured between the dominant slip direction and the foliation, is too small at a given shear strain, rather than being too large, as observed in the case of quartz textures.

Too large an angle between the a-axis maximum and the foliation during simple shear is only expected if the conjugate set corresponding to the weaker a-axis maximum operates in a synthetic sense ([26] and fig. 10, third sketch from the left). However, synthetic activity clearly cannot be expected in the case of near-symmetrical crossed girdles such as PT 463. Therefore, given the antithetical operation of the weaker of the two sets of favoured crystal orientations, too high an angle between the foliation and the stronger a-axis maximum must indicate a simultaneous stretch parallel to the SZB (fig. 10 sketch on the right).

Because asymmetrical crossed girdles are very widespread in mylonite belts we have to conclude that simple shear is exceedingly rare in mylonite belts. Hence, most mylonite belts may be regarded as "stretching shear zones", analogous to stretching faults [38], associated with simultaneous stretching in the wallrocks of the fault (respectively the "fault zone" in case of a mylonite belt). If, for example, the amount of stretching is greater in the footwall a systematic transition with increasing vorticity of flow towards the hangingwall may be observed across a mylonite belt, as documented for the Moine thrust [36].

### Conclusions

The few examples discussed make clear that further research is needed in order to gain additional insight into the mechanisms of texture formation. Observations on experimentally and naturally deformed rocks suggest that end-orientations for easy glide may form, particularly during simple shearing and in the presence of syntectonic recrystallization. On the other hand, it was concluded that simple shearing is very rare in mylonite belts.

It is certainly correct, however, that empirical arguments of essentially geometrical nature in favour of "low energy" (low CRSS) textures remain somewhat unsatisfactory [1]. The following lines of research are considered to be of prime importance in order to ultimately arrive at a more mechanistic interpretation of textures:

- (1) The results of computer modelling, experimental rock deformation and field studies need to be synthesized. It is not very fruitful to play one method off against the other.
- (2) Dynamic recrystallization obviously plays a key role in texture formation and must be taken into consideration by texture modelling work. The specific

recrystallization mechanism needs to be identified since different mechanisms might have different effects on the evolving texture.

(3) Many more laboratory experiments in simple shearing or along another strain path departing from axial shortening or extension are needed.

(4) Grain to grain interactions and the formation of fabric domains (as for example visualized by the "Achsenverteilungsanalyse") play a key role in texture formation. Methods such as the SEM electron channeling analysis [39] and misorientation imaging with optical methods [40] are extremely powerful in addressing this issue.

(5) In the case of field work, publications concerning applications of texture analysis by far outweigh the number of publications addressing processes of texture formation. More research is needed on well-documented monomineralic geological materials for which there is a maximum of independent evidence regarding the kinematics of deformation (strain path) and many other parameters such as for example temperature and active slip systems.

#### Acknowledgements

W. Skrotzki and J. Tullis are sincerely thanked for their careful review. My colleagues H. Stünitz and Ch. Pauli also helped to improve an early version of the manuscript.

#### References

- (1) H.-R. Wenk & J.M. Christie: Comments on the interpretation of deformation textures in rocks, *J. Struct. Geol.* 13 (1991), 1091-1110.
- (2) W. Schmidt: *Tektonik und Verformungslehre*, Bornträger, Berlin, 208pp.
- (3) G.S. Lister, M.S. Paterson & B.E. Hobbs: The simulation of fabric development during plastic deformation and its application to quartzite: The model, *Tectonophysics* 45 (1978), 107-158.
- (4) G.S. Lister & B.E. Hobbs: The simulation of fabric development during plastic deformation and its application to quartzite: the influence of deformation history, *J. Struct. Geol.* 2 (1980), 355-370.
- (5) H.-R. Wenk, C.R. Venkatasubramanian, D. Baker & F.J. Turner: Preferred orientation in experimentally deformed limestone, *Contr. Mineral. Petrol.* 38 (1973), 81-114.
- (6) H.-R. Wenk, G. Canova, A. Molinari & U.F. Kocks: Viscoplastic modelling of texture development in quartzite, *J. geophys. Res.* 94B (1989), 17895-17906.
- (7) A. Etchecopar: A plane kinematic model of progressive deformation in a polycrystalline aggregate, *Tectonophysics* 39 (1977), 121-139.
- (8) G.S. Lister: A vorticity equation for lattice reorientation during plastic deformation, *Tectonophysics* 82 (1982), 351-366.
- (9) A. Etchecopar & G. Vasseur: A 3D kinematic model of fabric development in polycrystalline aggregates: Comparisons with experimental and natural samples, *J. Struct. Geol.* 9 (1987), 705-717.
- (10) M.W. Jessell: Simulation of fabric development in recrystallizing aggregates - I. Description of the model, *J. Struct. Geol.* 10 (1988), 771-778.

- (11) M.W. Jessell: Simulation of fabric development in recrystallizing aggregates - II. Example model runs, *J. Struct. Geol.* 10 (1988), 779-793.
- (12) M.W. Jessell & G.S. Lister: A simulation of the temperature dependence of quartz fabrics, in: *Deformation Mechanisms, Rheology and Tectonics*, Spec. Publ. geol. Soc. Lond. 54 (1990), 353-362.
- (13) J.L. Bouchez & P. Duval: The fabric of polycrystalline ice deformed in simple shear: Experiments in torsion, natural deformation and geometrical interpretation, *Textures and Microstructures* 5 (1982), 171-190.
- (14) J.W. Glen: The mechanics of ice. Cold regions Research and Engineering Laboratory, Monograph II C2 (1975), Hannover, New Hampshire.
- (15) A. Higashi: Mechanisms of plastic deformation in ice single crystals, in: *Physics of Snow and Ice* 1 (1967), 277-289.
- (16) P.J. Huddleston: Progressive deformation and development of fabric across zones of shear in glacial ice, in: *Energetics of Geological Processes* (1977), Springer Verlag New York.
- (17) G.C. Gleason, J. Tullis & F. Heidelbach: The role of dynamic recrystallisation in the development of lattice preferred orientations in experimentally deformed quartz aggregates, *J. Struct. Geol.* 15 (1993), 1145-1168.
- (18) G. Hirth & J. Tullis: Dislocation creep regimes in quartz aggregates, *J. Struct. Geol.* 14 (1992), 145-159.
- (19) L.N. Dell'Angelo & J. Tullis: Fabric development in experimentally sheared quartzites, *Tectonophysics* 169 (1989), 1-21.
- (20) S. Ralser: Shear zones developed in an experimentally deformed quartz mylonite, *J. Struct. Geol.* 12 (1990), 1033-1045.
- (21) J.L. Bouchez, G.S. Lister & A. Nicolas: Fabric asymmetry and shear sense in movement zones, *Geol. Rundschau* 72 (1983), 401-419.
- (22) S.M. Schmid, R. Panozzo & S. Bauer: Simple shear experiments on calcite rocks: rheology and microfabric, *J. Struct. Geol.* 9 (1987), 747-778.
- (23) H.R. Wenk & H. Kern: Calcite texture development in experimentally induced ductile shear zones, *Contr. Miner. Petrol.* 83 (1983), 231-236.
- (24) J.H.P. DeBresser & C.J. Spiers: High-temperature deformation of calcite single crystals by r and f slip, in: *Deformation Mechanisms, Rheology and Tectonics*, Geol. Soc. Spec. Publ. 54 (1990), 285-298.
- (25) F.J. Turner & M. Orozco: Crystal bending in metamorphic calcite, and its relation to associated twinning, *Contr. Mineral. Petrol.* 57 (1976), 83-97.
- (26) N.S. Mancktelow: Quartz textures from the Simplon fault zone, southwest Switzerland and North Italy, *Tectonophysics* 135 (1987), 133-153.
- (27) H.R. Wenk, T. Takeshita, E. Bechler, B.G. Eskine & S. Matthies: Pure shear and simple shear calcite textures. Comparison of experimental, theoretical and natural data, *J. Struct. Geol.* 9 (1987), 731-745.
- (28) R.D. Law: Crystallographic fabrics: a selective review of their applications to research in structural geology, in: *Deformation Mechanisms, Rheology and Tectonics*, Geol. Soc. Spec. Publ. 54 (1990), 335-352.
- (29) W.D. Means: Kinematics, stress, deformation and material behaviour, *J. Struct. Geol.* 12 (1990), 953-971.
- (30) S.M. Schmid & M. Casey: Complete fabric analysis of some commonly observed quartz c-axis patterns, *Geophysical Monograph* 36 (1986), 263-286.
- (31) J.-L. Bouchez: Preferred orientations of quartz a axes in some tectonites: kinematic inferences, *Tectonophysics* 49 (1978), T25-T30.

- (32) S.M. Schmid, M. Casey & J. Starkey: An illustration of the advantages of a complete texture analysis described by the orientation distribution function (ODF) using quartz pole figure data, *Tectonophysics* 78 (1981), 101-117.
- (33) P. Blumenfeld, D. Mainprice & J.-L. Bouchez: C-slip in quartz from subsolidus deformed granite, *Tectonophysics* 127 (1986), 97-115.
- (34) R.D. Law, S.M. Schmid & J. Wheeler: Simple shear deformation and quartz crystallographic fabrics: a possible natural example from the Torridon area of NW Scotland, *J. Struct. Geol.* 12 (1990), 29-45.
- (35) B. Sander: Einführung in die Gefügekunde der geologischen Körper, zweiter Teil: Die Korngefüge (1950), Springer-Verlag Wien, 409pp.
- (36) R. Law: Heterogeneous deformation and quartz crystallographic fabric transitions: natural examples from the Stack of Glencoul, northern Assynt, *J. Struct. Geol.* 9 (1987), 819-833.
- (37) J.P. Platt & J.H. Behrmann: Structures and fabrics in a crustal scale shear zone, Betic Cordilleras, SE Spain, *J. Struct. Geol.* 8 (1986), 15-34.
- (38) W.D. Means: Stretching faults, *Geology* 17 (1989), 893-896.
- (39) G.E. Lloyd & B. Freeman: SEM electron channelling analysis of dynamic recrystallization in a quartz grain, *J. Struct. Geol.* 13 (1991), 945-953.
- (40) R. Panozzo Heilbronner & C. Pauli: Integrated spatial and orientation analysis of quartz c-axes by computer-aided microscopy, *J. Struct. Geol.* 15 (1993), 369-382.